DOI: http://doi.org/10.25728/cs.2023.1.5

MANAGING THE HANDLING–COMFORT TRADE-OFF IN THE FULL CAR MODEL BY ACTIVE SUSPENSION CONTROL

M. Alhelou[1], Y. Wassouf[2], M.V. Korzhukov[3], E.S. Lobusov[4], and V.V. Serebrenny[5]

[1,2,4,5]Bauman Moscow State Technical University, Moscow, Russia
[2,3]KAMAZ Innovation Center, Moscow, Russia

[1]✉ muhammed.alhelou@gmail.com [2]✉ vassufya@student.bmstu.ru [3]✉ KorzhukovMV@kamaz.ru
[4]✉ evgeny.lobusov@yandex.ru [5]✉ vsereb@bmstu.ru

Abstract. The effectiveness of a car suspension is usually assessed by the ability to provide maximum ride comfort and maintain continuous contact of the wheels with the road (road holding). This paper develops an active suspension control algorithm for the full car model (FCM) to improve its characteristics by active disturbance rejection control (ADRC). The ride comfort and road holding characteristics of the FCM suspension system are compared with those of the passive suspension. We propose an optimization algorithm for managing the handling–comfort trade-off using a single variable. This algorithm is based on forecasting the future values of the car chassis displacement and the roll angle depending on the dynamics of the ADRC controller on a given horizon. The simulation results confirm the effectiveness of the active suspension system with the proposed algorithm in improving the ride comfort and road holding characteristics.

Keywords: active disturbance rejection control (ADRC), full car model (FCM), extended state observer, ride comfort, handling, PD controller, tracking differentiator.

INTRODUCTION

Suspension is one of the few car systems that have significant disadvantages [1]. Vehicle designers, engineers, and researchers put a lot of effort into improving vehicle suspension control systems. The most serious challenge for suspension operation is the need to increase ride comfort without losing stability and road holding [2, 3].

The ride comfort problem is to isolate passengers, as much as possible, from the vertical accelerations due to the interaction of the car wheels with the road. The road holding problem is to maintain maximum wheel contact with the road surface. When a wheel falls into a bump or pothole, it causes a significant reaction force to increase contact with the road surface. This maintains different handling levels at every time of the car's movement.

The handling problem is to find a balance between two characteristics: ride comfort and road holding. When the springs of a suspension system are too stiff or too soft, the suspension does not work effectively because it cannot optimally isolate the vehicle from irregularities of the road surface. A soft suspension provides good ride comfort, whereas a stiff suspension provides good road holding. Suspension stiffness must be adjusted between the extreme values to ensure good handling.

There is an inherent conflict between ride comfort and suspension deflection since the wheel position roughly corresponds to the road profile at low frequencies (< 5rad/s): any reduction in body travel at these frequencies will increase suspension deflection [4]. In this regard, it is topical to trade off between these two characteristics.

A common way to manage this trade-off is to provide ride comfort when the relative displacement between the sprung and unsprung masses (suspension travel) exceeds the suspension travel limits. The system regulator restricts the suspension travel to settle the handling issue under the limit values [5].

A set of mechanical solutions was proposed to resolve the conflict between ride comfort and handling. One of them was described in the paper [6]. The cited authors suggested design criteria for a semi-active suspension system to reduce significantly or even eliminate the conflict between ride comfort and handling. The operation of the system depends on switching between a stiff spring at the high damping mode (to ensure handling) and a soft spring at the low damping mode (to ensure ride comfort). However, many mechanical solutions directly involve the driver because an appropriate operation mode must be determined based on the road terrain.

In [7], genetic algorithms were used to optimize several car movement indicators under constraints. However, such a system must have a mode switching mechanism during operation.

The paper [8] considered the simulation and control of an active suspension system for the full car model. A *linear quadratic regulator* (LQR) was proposed to ensure ride comfort or road handling. The control system was tested on bumps of different heights. The test results showed good effectiveness of the control system. However, it has no mode switching mechanism.

The authors [9–11] used *model predictive control* (MPC) to ensure the high quality of operation of several car systems, particularly to improve ride comfort and handling. The input constraints of the control system, the system state, and the information coming from the preview system were considered. However, the operation of this system needs a large set of predictive data and computations. The MPC-based optimization procedure may be too long-lasting to function in real time.

A reliable control method for the active suspension system was developed in [12–14]. The effect of the road relief and obstacles on the car and passengers was minimized using H_∞ controllers. Nevertheless, the proposed method can be extended to focus on the handling problem. The conflict between comfort and handling can be eliminated by introducing a positive variable, but it will considerably increase the controller's dimension. As a result, the controller's tuning procedure will also require more effort.

In previous publications (for example, see [15] and [16]), we applied data-driven methods (active rejection disturbance control, ARDC) to manage the handling–comfort trade-off.

This paper focuses on managing the conflict between ride comfort and handling using ARDC. For this purpose, we propose a new optimization approach: minimize a quality index to solve both problems by means of one parameter.

1. THE FULL CAR MODEL

Figure 1 shows a car model with an active suspension with 7 degrees of freedom.

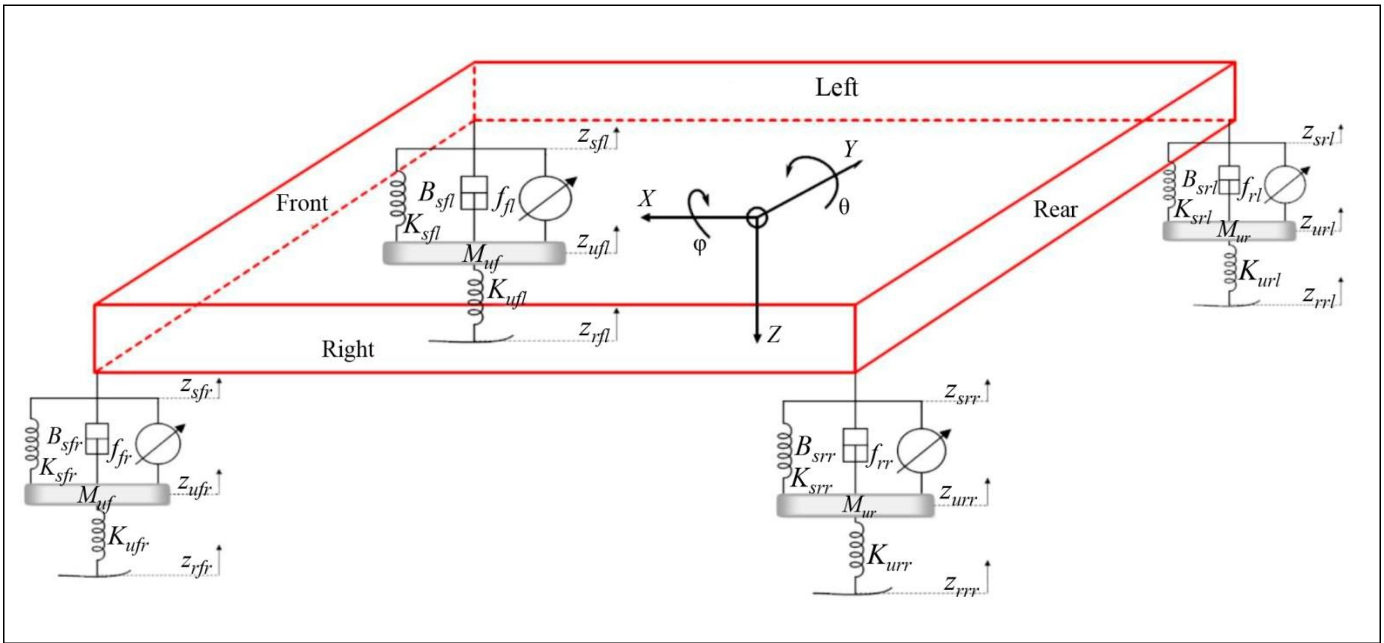

Fig. 1. The car model with active suspension and 7 degrees of freedom.

This model includes the characteristics of the heave, pitch, and roll of the suspension mass and the vertical displacements of the front and rear suspensions. For simplicity of calculations and modeling, all pitch and roll angles are assumed small. The suspension model is described by linear spring elements with a shock absorber; the tires are modeled as simple linear springs without shock absorbers. To simplify the presentation, we divide the vehicle's dynamics equations into three parts:

- the unsprung mass equations, which describe the vertical accelerations of the car wheels in terms of suspension deflections and road disturbances:

$$\begin{aligned}
m_u\ddot{z}_{ufl} &= K_{sf}\left(z_{sfl}-z_{ufl}\right)+B_{sfl}\left(\dot{z}_{sfl}-\dot{z}_{ufl}\right)\\
&\quad -K_u\left(z_{ufl}-z_{rfl}\right)-f_{fl},\\
m_u\ddot{z}_{ufr} &= K_{sf}\left(z_{sfr}-z_{ufr}\right)+B_{sfr}\left(\dot{z}_{sfr}-\dot{z}_{ufr}\right)\\
&\quad -K_u\left(z_{ufr}-z_{rfr}\right)-f_{fr},\\
m_u\ddot{z}_{url} &= K_{sr}\left(z_{srl}-z_{url}\right)+B_{srl}\left(\dot{z}_{srl}-\dot{z}_{url}\right)\\
&\quad -K_u\left(z_{url}-z_{rrl}\right)-f_{rl},\\
m_u\ddot{z}_{urr} &= K_{sr}\left(z_{srr}-z_{urr}\right)+B_{srr}\left(\dot{z}_{srr}-\dot{z}_{urr}\right)\\
&\quad -K_u\left(z_{urr}-z_{rrr}\right)-f_{rr};
\end{aligned}\tag{1}$$

- the chassis angle equations, which describe the relationship between the vertical displacement of the vehicle chassis at each angle with all system states:

$$\begin{aligned}
z_{sfl} &= w_f\phi+a\theta+z_s,\\
z_{sfr} &= -w_f\phi+a\theta+z_s,\\
z_{srl} &= w_r\phi-b\theta+z_s,\\
z_{srr} &= -w_r\phi-b\theta+z_s,
\end{aligned}$$

where w is the car width and a and b are the approximate distances from the car's center of mass to the front and rear, respectively;

- the sprung mass equations, which describe the vertical acceleration of the car chassis and the linear accelerations of the roll and pitch angles:

$$\begin{aligned}
m_s\ddot{z}_s &= -K_{sf}\left(z_{sfl}-z_{ufl}\right)-K_{sf}\left(z_{sfr}-z_{ufr}\right)-\\
&\quad -K_{sr}\left(z_{srl}-z_{url}\right)-\ldots-K_{sr}\left(z_{srr}-z_{urr}\right)-\\
&\quad -B_{sfl}\left(\dot{z}_{sfl}-\dot{z}_{ufl}\right)-B_{sfr}\left(\dot{z}_{sfr}-\dot{z}_{ufr}\right)-\ldots.\\
&\quad -B_{srl}\left(\dot{z}_{srl}-\dot{z}_{url}\right)-B_{srr}\left(\dot{z}_{srr}-\dot{z}_{urr}\right)+\\
&\quad +f_{fl}+f_{fr}+f_{rl}+f_{rr},\\
I_{yy}\ddot{\theta} &= -aK_{sf}\left(z_{sfl}-z_{ufl}\right)-aK_{sf}\left(z_{sfr}-z_{ufr}\right)+\\
&\quad +bK_{sr}\left(z_{srl}-z_{url}\right)+bK_{sr}\left(z_{srr}-z_{urr}\right)-\\
&\quad -aB_{sfl}\left(\dot{z}_{sfl}-\dot{z}_{ufl}\right)-aB_{sfr}\left(\dot{z}_{sfr}-\dot{z}_{ufr}\right)+\\
&\quad +bB_{srl}\left(\dot{z}_{srl}-\dot{z}_{url}\right)+bB_{srr}\left(\dot{z}_{srr}-\dot{z}_{urr}\right)+\ldots\\
&\quad +af_{fl}+af_{fr}-bf_{rl}-bf_{rr},\\
I_{xx}\ddot{\varphi} &= -w_fK_{sf}\left(z_{sfl}-z_{ufl}\right)+w_fK_{sf}\left(z_{sfr}-z_{ufr}\right)-\\
&\quad -w_rK_{sr}\left(z_{srl}-z_{url}\right)+w_rK_{sr}\left(z_{srr}-z_{urr}\right)-\\
&\quad -w_fB_{sfl}\left(\dot{z}_{sfl}-\dot{z}_{ufl}\right)+w_fB_{sfr}\left(\dot{z}_{sfr}-\dot{z}_{ufr}\right)-\\
&\quad -w_rB_{srl}\left(\dot{z}_{srl}-\dot{z}_{url}\right)+w_rB_{srr}\left(\dot{z}_{srr}-\dot{z}_{urr}\right)+\ldots\\
&\quad +w_ff_{fl}-w_ff_{fr}+w_rf_{rl}-w_rf_{rr}.
\end{aligned}\tag{2}$$

The state variables of the system are described in Table 1, and the parameter values of the system are given in Table 2. The equations, state variables, and parameters are taken from [17].

Table 1

State variables for the full car model

Notation	Description
z	Heave position (ride height of sprung mass)
θ	Pitch angle
ϕ	Roll angle
z_{sfl}, z_{ufl}	Left-front wheel sprung/unsprung mass displacement
z_{sfr}, z_{ufr}	Right-front wheel sprung/unsprung mass displacement
z_{srl}, z_{url}	Left-rear wheel sprung/unsprung mass displacement
z_{srr}, z_{urr}	Right-rear wheel sprung/unsprung mass displacement
f_{fl}	Left-front control force
f_{fr},	Right-front control force
f_{rl}	Left-rear control force
f_{rr}	Right-rear control force

Table 2

Parameter values of the full car model

Notation	Description	Value
m_s	Mass of vehicle body (sprung mass)	1500 kg
m_u	Mass of wheel (unsprung mass)	59 kg
$K_{sf} = K_{sfl} = K_{sfr}$	Stiffness of vehicle body suspension spring for front	35 000 N/m
$K_{sr} = K_{srl} = K_{srr}$	Stiffness of vehicle body suspension spring for rear	38 000 N/m
K_u	Tire spring stiffness	190 000 N/m
$B_{sf} = B_{sfl} = B_{sfr}$	Front suspension damping	1000 N·s/m
$B_{sr} = B_{srl} = B_{srr}$	Rear suspension damping	1100 N·s/m
I_{xx}	Roll axis moment of inertia of vehicle body	460 kg·m^2
I_{yy}	Pitch axis moment of inertia of vehicle body	2160 kg·m^2

2. PROBLEM STATEMENT

The proposed approach is developed on a modeling platform with an ARM microcontroller, a simple platform created by the authors. (It contains a microcontroller, a USB port, and a power source.) Low-cost sensors commonly used in commercial products are connected to the microcontroller. This platform is used to control fast active suspensions.

Four different types of sensors are employed: accelerometers, gyroscopes, magnetometers, and potentiometers. They are connected through an Ethernet network to a central control unit. The Ethernet connection is important because it guarantees the modular architecture of the control system: individual units can be connected or disconnected without reducing the data transfer rate.

Figure 2 shows the arrangement of the sensors: four linear potentiometers are mounted on the suspensions along with a set of eight triaxial MEMS accelerometers (four on the wheels and four on the car body frame, near the suspension joint). An *inertial measurement unit* (IMU) with 9 degrees of freedom consists of a three-axis accelerometer, a three-axis gyroscope, and a three-axis magnetometer. This unit is mounted near the car's center of gravity. The four sensors located on the frame perform two tasks: they measure vertical accelerations near the suspension location and assist in estimating the overall position of the vehicle. The four values of the 3D acceleration from the four nodes are transmitted to the IMU to better estimate the vehicle's pitch and roll angles.

Due to a small amount of information about the system dynamics, the IMU 9 DOF sensor is employed to estimate the pitch, roll, and yaw angles using *the gradient descent algorithm*. Four potentiometers at each corner of the car are employed to measure suspension deflections. The accelerometers on each wheel and each corresponding angle chassis are employed to

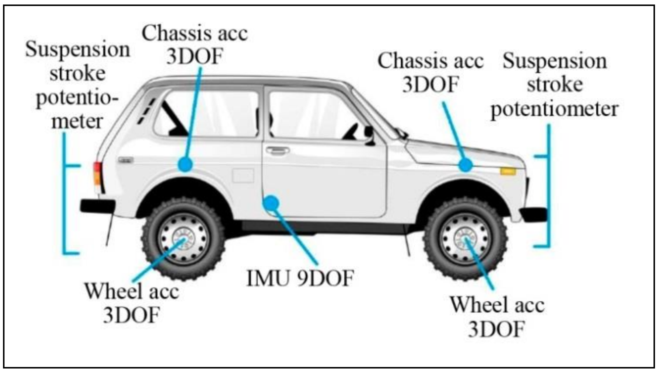

Fig. 2. The arrangement of sensors on the vehicle.

estimate *the dynamic load coefficient* (DLC) of each wheel. This is done as follows.

Summing the dynamic equations of the quarter-car system sequentially yields the equation

$$\left.\begin{aligned} &\frac{m_s}{4}\ddot{z}_{si} = -K_{si}z_{si} - C_{si}\dot{z}_{si} + u_i \\ &m_{ui}\ddot{z}_{ui} = K_{si}z_{si} + C_{si}\dot{z}_{si} - K_u\left(z_{ui} - z_{ri}\right) - u_i \end{aligned}\right\} \Rightarrow$$

$$\frac{m_s}{4}\ddot{z}_{si} + m_u\ddot{z}_{ui} = -K_u\left(z_{ui} - z_{ri}\right);\ i \in \{fl,\ fr,\ rl,\ rr\}.$$

As a result,

$$DLC_i = RMS\left(\frac{K_u(z_{ui} - z_{ri})}{(m_{si} + m_u)g}\right) = RMS\left(-\frac{\left(m_s/4\right)\ddot{z}_{si} + m_u\ddot{z}_{ui}}{\left(\left(m_s/4\right) + m_u\right)g}\right)$$

with the following notations: C_{si} is the suspension damping rate of the ith wheel; z_{ui} is the vertical displacement of the ith wheel; z_{si} is the vertical displacement of the ith node chassis; z_{ri} is the road noise in the ith node; finally, RMS is the root mean square value.

Figure 3 presents the data acquisition scheme for feedback control.

According to [12], the degrees of ride comfort and handling can be described by the acceleration of the vehicle's center of gravity and the roll angle, respectively. The degree of ride comfort is assessed by the index

$$\sigma_1 = RMS(\ddot{z}_s), \tag{3}$$

where $\ddot{z}_s$ denotes the acceleration of the sprung mass of the entire vehicle body.

The degree of handling is assessed by the index

$$\sigma_2 = \sqrt{\int_{0Hz}^{20Hz} S_\varphi . dw \times \frac{\sum_{i=1}^{4} DLC_i}{4}}, \tag{4}$$

where DLC_i denotes the dynamic load rate at the ith corner of the vehicle and S_φ is *the power spectral density* (PSD) of the roll angle.

Each wheel of the car is equipped with a hydraulic fast-response actuator. Figure 4 shows the suspension system on one wheel.

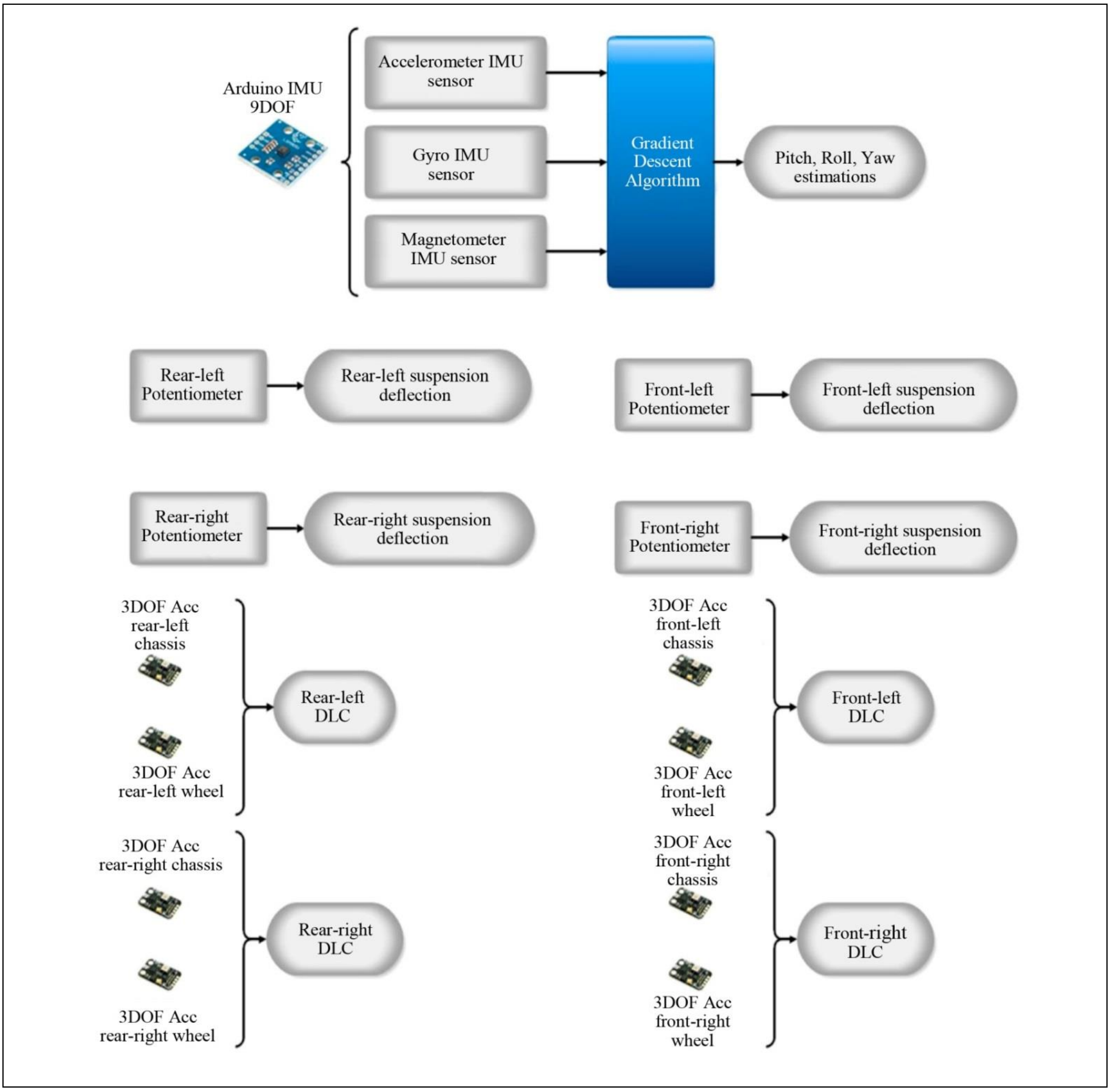

Fig. 3. The data acquisition scheme.

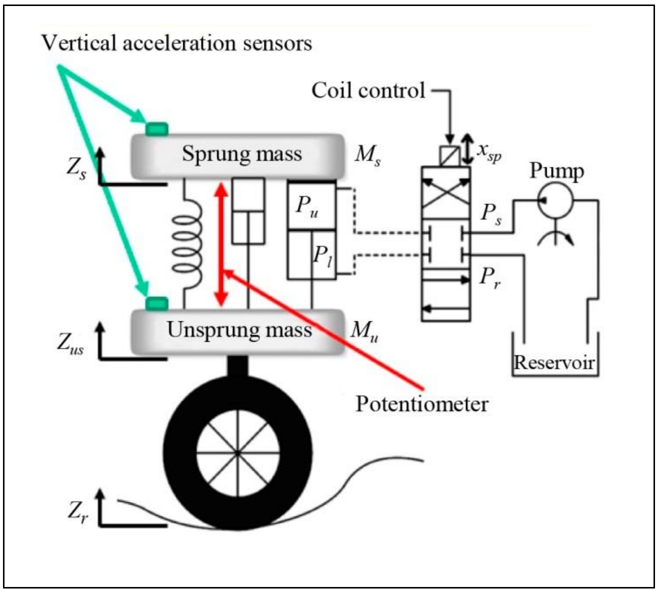

Fig. 4. Active hydraulic drive.

The hydraulic actuator consists of a spool (servo) valve and a hydraulic cylinder. Figure 4 has the following notations: P_s and P_r are the pressure of the hydraulic fluid entering and leaving the spool valve, respectively; x_{sp} is the position of the spool valve; P_u and P_l are the oil pressure in the upper and lower cylinder chambers, respectively; Z_u is the vertical wheel displacement; Z_s is the vertical chassis displacement; finally, Z_r is the road noise.

When the spool valve moves upwards (positive value), the upper chamber of the cylinder is connected to the supply line and its pressure increases. Meanwhile, the lower chamber is connected to the discharge line and its pressure decreases. The resulting pressure drop causes the cylinder piston to extend or retract.

For the mechanical movement of the valve spool, an electric current is applied to the coil connected to the servo valve. The powered actuator drives the spool to the desired position. The actuator dynamics equation can be found in [18].

It is required to find a control law and its parameters affecting the degrees of handling and suspension damping (ride comfort). The following conditions must be satisfied:

- The control system must be built using observations.
- A certain relation between the degrees of suspension damping and handling must be ensured depending on the current conditions (driving up to 70 km/h on Class D roads according to the ISO 8608 standard).

The next section briefly describes a control algorithm for the vehicle's suspension system based on active disturbance rejection control (ADRC). ADRC is a class of control systems intended to suppress disturbances. The algorithm operates under conditions where the complete model of a plant (e.g., the actuator) is unknown and the observer eliminates the uncertainties due to insufficient information.

3. THE LINEAR ACTIVE DISTURBANCE REJECTION CONTROL SCHEME OF THE SECOND ORDER

Linear active disturbance rejection control (LADRC) is based on the generalized ADRC approach [19]. Figure 5 presents the LADRC scheme of the second order.

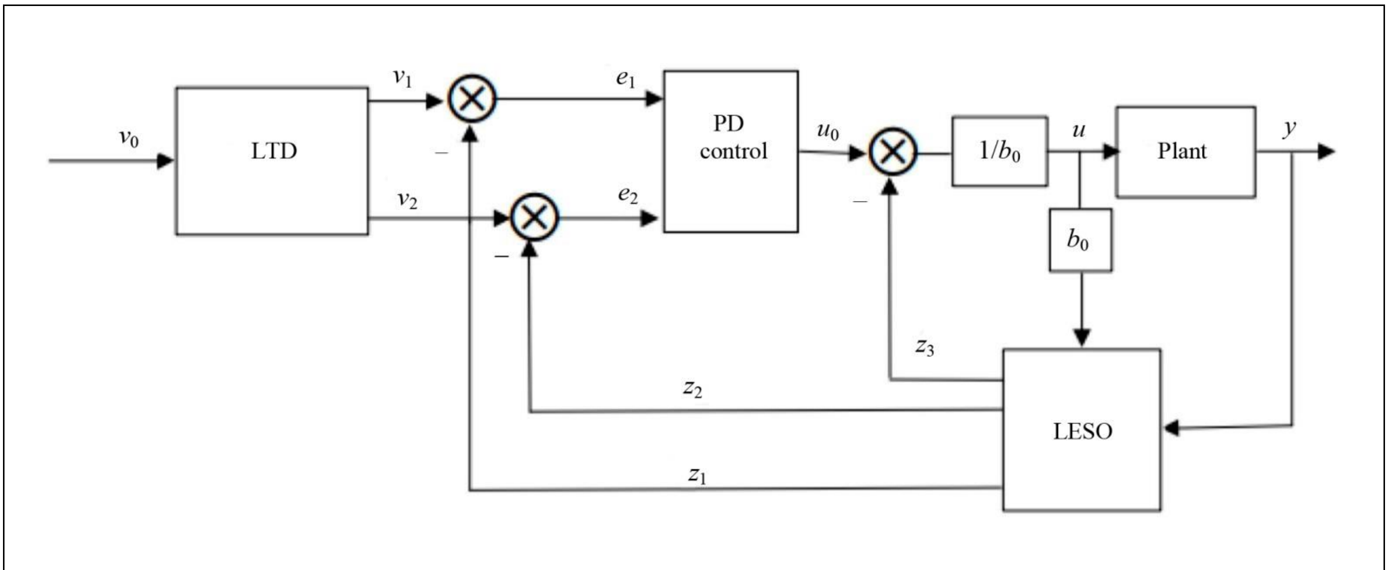

Fig. 5. The LADRC scheme of the second order.

The ADRC system consists of two main loops (feedback and estimation) and contains four main blocks (a controller, a linear extended state observer (LESO), a linear tracking differentiator (LTD), and a disturbance rejection scheme).

3.1. Linear tracking differentiator

An LTD is a pre-filter that processes an input signal and its rate of change.

The input signal is smoothed by an LTD. Its outputs are two signals: a pre-filtered useful signal and its rate of change. The algorithm has the following form:

$$\dot{v}_1 = v_2,$$
$$\dot{v}_2 = -k_1(v_1 - v_0) - k_2 v_2,$$

where v_0 is a useful signal, v_1 is the filtered useful signal, v_2 is its rate of change, and k_1 and k_2 are the adjustable LTD parameters. In the case $k_1 = r^2, k_2 = 2r, r > 0,$ there is no overshoot and the transient time approximately equals $T_0 = 7/r$, where the coefficient r characterizes the rate of change of the filtered useful signal.

Thus, an LTD simultaneously controls the reference signal and its rate of change. In this paper, we do not apply LTDs: the useful signal is always 0.

3.2. Linear extended state observer

An extended state observer (ESO) obtains information about generalized disturbances (uncertainties and external disturbances $\hat{f}$ and internal system dynamics $\hat{y}$ and $\dot{\hat{y}}$).

Thus, a simple Luenberger observer can be used to estimate the general disturbances of the system and its states; see the details below.

The system dynamics can be written as

$$\ddot{y} = g(t, y, \dot{y}) + b_0 u + w \tag{5}$$

with the following notations: y is the output signal; u is the control action; $g(\cdot)$ is a function describing the plant dynamics (including the unknown dynamics); w is an external disturbance; finally, b_0 is the system coefficient. The system dynamics components ($g(\cdot)$, b_0, and w) are often not exactly known. By combining the external and internal disturbances in one function $f(\cdot)$, we represent the system as

$$\ddot{y} = f(t, y, \dot{y}, w) + b_0 u. \tag{6}$$

The state-space form of equation (6) is given by

$$\dot{x}_1 = x_2,$$
$$\dot{x}_2 = f + b_0 u,$$
$$y = x_1.$$

The general disturbance is introduced as follows:

$$\dot{x}_1 = x_2,$$
$$\dot{x}_2 = x_3 + au,$$
$$\dot{x}_3 = \dot{f}(t, x_1, x_2, w),$$
$$y = x_1.$$

We write the last equations in the state space:

$$\dot{x} = A_x x + B_x u + E_x \dot{f},$$
$$y = C_x x,$$

where

$$A_x = \begin{bmatrix} 0 & 1 & 0 \\ 0 & 0 & 1 \\ 0 & 0 & 0 \end{bmatrix}, B_x = \begin{bmatrix} 0 \\ b_0 \\ 0 \end{bmatrix},$$
$$C_x = \begin{bmatrix} 1 & 0 & 0 \end{bmatrix}, E_x = \begin{bmatrix} 0 \\ 0 \\ 1 \end{bmatrix}.$$

The linear extended state observer (LESO) may serve to estimate the states x_1, x_2, and x_3. Thus, the LESO can be represented as

$$\dot{z}_1 = z_2 - \alpha_1 \hat{e},\ \dot{z}_2 = z_3 + \widehat{b}_0 u - \alpha_2 \hat{e},\ \dot{z}_3 = -\alpha_3 \hat{e}$$

with the following notations: z_1, z_2, and z_3 are the approximated values of the states x_1, x_2, and x_3, respectively; α_1, α_2, and α_3 are the observer coefficients; $\hat{e} = y - z_1$ is the error estimate; finally, $\widehat{b}_0$ is the approximated value of the coefficient b_0 in equation (1), which can be chosen empirically.

The observed variables ($\hat{y} = z_1$, $\dot{\hat{y}} = z_2$, and $\hat{f} = z_3$) along with the approximated value $\widehat{b}_0$ are used to reject the disturbances and control the system; see Fig. 5.

3.3. Disturbance rejection scheme

This scheme can be defined as follows:

$$u = \frac{u_0 - z_3}{\widehat{b}_0} = \frac{u_0 - \hat{f}}{\widehat{b}_0},$$

where u_0 denotes the controller's output.

Let us return to equation (6) and replace u by its calculated value:

$$\ddot{y} = f(\cdot) + b_0\left(\frac{u_0 - \hat{f}}{\hat{b}_0}\right).$$

Assume that by the observation results, $\hat{b}_0 \approx b_0$ and $\hat{f} \approx f$. Then the dynamic equation takes the form

$$\ddot{y} \approx u_0 .$$

3.4. Feedback controller

Let the feedback controller be a proportional-differential (PD) controller. In this case, the control signal u_0 can be written as

$$u_0(t) = K_p(y_{ref} - \hat{y}) + K_d\dot{\hat{y}}.$$

We choose the coefficients of the PD controller as follows:

$$K_p = w_{CL}^2, \quad K_d = -2\xi w_{CL},$$

where w_{CL} and ξ are the desired pole and damping factor of the closed loop system, respectively.

The observer's poles w_{ESO} must be placed to the left at a distance exceeding n times the closed-loop pole:

$$w_{ESO} = nw_{CL}, \; n \in [3, 10].$$

This placement ensures sufficiently fast dynamics of the observer.

For simplicity, let all poles be equal. Therefore, the characteristic equation of the observer takes the form

$$D(\lambda) = (\lambda - w_{ESO})^3$$
$$= \lambda^3 - 3w_{ESO}\lambda^2 - 3w_{ESO}^2\lambda - w_{ESO}^3.$$

The coefficients $\alpha_1, \alpha_2,$ and α_3 are calculated by solving the equation

$$D(\lambda) = |sI - A_x + LC_x|,$$

where

$$I = \begin{bmatrix} 1 & 0 & 0 \\ 0 & 1 & 0 \\ 0 & 0 & 1 \end{bmatrix}, \; L = \begin{bmatrix} \alpha_1 \\ \alpha_2 \\ \alpha_3 \end{bmatrix}.$$

As a result, the observer coefficients are chosen as follows:

$$\alpha_1 = -3w_{ESO}, \; \alpha_2 = -3w_{ESO}^2, \; \alpha_3 = -w_{ESO}^3.$$

Remark. This paper considers three control variables, namely, the roll and pitch angles and the vertical displacement of the chassis. Each of these channels is controlled by an independent ADRC law and is described by the general equation (5).

4. AN APPROACH BASED ON OPTIMIZED ADRC

If control aims at minimizing the vertical displacement z_s of the sprung mass, the vertical acceleration will also be minimized, providing the necessary ride comfort. Thus, the handling–comfort trade-off can be interpreted as a balance between the body displacement z_s and the roll angle φ.

Then the quality criterion to optimize the performance of the suspension system is defined by

$$J = \int_0^{T_p} \left[(1-\rho)(\varphi(t+\tau))^2 + \rho(z_s(t+\tau))^2\right] d\tau, \qquad (7)$$

where T_p is the optimization horizon, $z_s(t+\tau)$ is the future vertical displacement of the chassis after some time τ, and $\varphi(t+\tau)$ is the future roll angle.

The future values are forecasted by expanding the functions $z_s(t+\tau)$ and $\varphi(t+\tau)$ into Taylor series:

$$\begin{aligned} z_s(t+\tau) &\approx z_s(t) + \tau\dot{z}_s(t) + \frac{\tau^2}{2}\ddot{z}_s(t), \\ \varphi(t+\tau) &\approx \varphi(t) + \tau\dot{\varphi}(t) + \frac{\tau^2}{2}\ddot{\varphi}(t). \end{aligned} \qquad (8)$$

The second derivatives of the output parameters are estimated using the basic dynamic equation of the ADRC system:

$$\begin{aligned} \hat{\ddot{z}}_s &= b_z\hat{u}_z + \hat{f}_z, \\ \hat{\ddot{\varphi}} &= b_\varphi\hat{u}_\varphi + \hat{f}_\varphi. \end{aligned} \qquad (9)$$

Substituting equations (9) into equations (8) yields

$$\hat{z}_s(t+\tau) \approx \mathcal{T}(\tau)(\hat{X}_z + \hat{U}_z),$$
$$\hat{\varphi}(t+\tau) \approx \mathcal{T}(\tau)(\hat{X}_\varphi + \hat{U}_\varphi),$$

where

$$\mathcal{T} = \begin{bmatrix} 1 & \tau & \frac{\tau^2}{2} \end{bmatrix}, \; \hat{X}_z = \begin{bmatrix} z_s & \dot{z}_s & \hat{f}_z \end{bmatrix}^{\mathrm{T}},$$
$$\hat{U}_z = \begin{bmatrix} 0 & 0 & b_z\hat{u}_z \end{bmatrix}^{\mathrm{T}},$$
$$\hat{X}_\varphi = \begin{bmatrix} \varphi & \dot{\varphi} & \hat{f}_\varphi \end{bmatrix}^{\mathrm{T}}, \text{ and } \hat{U}_\varphi = \begin{bmatrix} 0 & 0 & b_\varphi\hat{u}_\varphi \end{bmatrix}^{\mathrm{T}}.$$

As a result, the quality criterion becomes

$$J = \int_0^{T_p} \rho[\mathcal{T}(\tau)(\hat{X}_z + \hat{U}_z)]^2$$
$$+ (1-\rho)[\mathcal{T}(\tau)(\hat{X}_\varphi + \hat{U}_\varphi)]^2 d\tau.$$

We transform equation (7) to

$$J=\frac{\rho}{2}[\hat{X}_z^{\mathrm{T}}+\hat{U}_z^{\mathrm{T}}]\mathcal{T}_s[(\hat{X}_z+\hat{U}_z)]$$
$$+\frac{1-\rho}{2}[\hat{X}_\varphi^{\mathrm{T}}+\hat{U}_\varphi^{\mathrm{T}}]\mathcal{T}_s[\hat{X}_\varphi^{\mathrm{T}}+\hat{U}_\varphi],$$

where

$$\mathcal{T}_s=\int_0^{T_p}\mathcal{T}^{\mathrm{T}}(\tau)\mathcal{T}(\tau)d\tau=\begin{bmatrix} T_p & \frac{T_p^2}{2} & \frac{T_p^3}{6} \\ \frac{T_p^2}{2} & \frac{T_p^3}{3} & \frac{T_p^4}{8} \\ \frac{T_p^3}{6} & \frac{T_p^4}{8} & \frac{T_p^5}{20} \end{bmatrix}$$
$$=\begin{bmatrix} T_{11} & T_{12} \\ T_{21} & T_{22} \end{bmatrix}.$$

Let us denote $\hat{X}_{1z}=[z_s,\ \dot{z}_s]^{\mathrm{T}}$, $\hat{X}_{2z}=\hat{f}_z$, $\hat{U}_{2z}=b_z\hat{u}_z$, $\hat{X}_{1\varphi}=[\varphi,\ \dot{\varphi}]^{\mathrm{T}}$, $\hat{X}_{2\varphi}=\hat{f}_\varphi$, and $\hat{U}_{2\varphi}=b_\varphi\hat{u}_\varphi$. Then the quality criterion takes the form

$$J=\frac{\rho}{2}\begin{pmatrix}\hat{X}_{1z}^{\mathrm{T}} & \hat{X}_{2z}^{\mathrm{T}}+\hat{U}_{2z}^{\mathrm{T}}\end{pmatrix}\begin{pmatrix} T_{11} & T_{12} \\ T_{21} & T_{22} \end{pmatrix}\begin{pmatrix}\hat{X}_{1z} \\ \hat{X}_{2z}+\hat{U}_{2z}\end{pmatrix}$$
$$+\ldots+\frac{1-\rho}{2}\begin{pmatrix}\hat{X}_{1\varphi}^{\mathrm{T}} & \hat{X}_{2\varphi}^{\mathrm{T}}+\hat{U}_{2\varphi}^{\mathrm{T}}\end{pmatrix}\begin{pmatrix} T_{11} & T_{12} \\ T_{21} & T_{22} \end{pmatrix}\begin{pmatrix}\hat{X}_{1\varphi} \\ \hat{X}_{2\varphi}+\hat{U}_{2\varphi}\end{pmatrix}.$$

Consequently, its partial derivatives with respect to the control variable are

$$\frac{\partial J}{\partial \hat{U}_{2z}}=\frac{\rho}{2}\left(T_{12}^{\mathrm{T}}\hat{X}_{1z}+T_{22}^{\mathrm{T}}\hat{X}_{2z}+T_{21}\hat{X}_{1z}\right.$$
$$\left.+T_{22}\hat{X}_{2z}+2T_{22}\hat{U}_{2z}\right),$$
$$\frac{\partial J}{\partial \hat{U}_{2\varphi}}=\frac{1-\rho}{2}\left(T_{12}^{\mathrm{T}}\hat{X}_{1\varphi}+T_{22}^{\mathrm{T}}\hat{X}_{2\varphi}\right.$$
$$\left.+T_{21}\hat{X}_{1\varphi}+T_{22}\hat{X}_{2\varphi}+2T_{22}\hat{U}_{2\varphi}\right).$$

Due to $T_{12}^{\mathrm{T}}=T_{21}$ and $T_{22}^{\mathrm{T}}=T_{22}$, these expressions can be simplified to

$$\frac{\partial J}{\partial \hat{U}_{2z}}=\rho\left(T_{21}\hat{X}_{1z}+T_{22}(\hat{X}_{2z}+\hat{U}_{2z})\right),$$
$$\frac{\partial J}{\partial \hat{U}_{2\varphi}}=(1-\rho)\left(T_{21}\hat{X}_{1\varphi}+T_{22}(\hat{X}_{2\varphi}+\hat{U}_{2\varphi})\right).$$

If the control is $\hat{U}_2=\begin{bmatrix}\rho\hat{U}_{2z} \\ (1-\rho)\hat{U}_{2\varphi}\end{bmatrix}$, the optimal control will satisfy $\frac{\partial J}{\partial \hat{U}_2}=0$, i. e.,

$$\begin{bmatrix}\frac{\partial J}{\partial \hat{U}_{2z}}=0 \\ \frac{\partial J}{\partial \hat{U}_{2\varphi}}=0\end{bmatrix}.$$

Thus,

$$T_{22}\hat{U}_{2z}=-T_{21}\hat{X}_{1z}-T_{22}\hat{X}_{2z},$$
$$T_{22}\hat{U}_{2\varphi}=-T_{21}\hat{X}_{1\varphi}-T_{22}\hat{X}_{2\varphi}.$$

This leads to the following control law:

$$\hat{U}_{2z}=-\left(T_{22}\right)^{-1}T_{21}\hat{X}_{1z}-\hat{X}_{2z},$$
$$\hat{U}_{2\varphi}=-\left(T_{22}\right)^{-1}T_{21}\hat{X}_{1\varphi}-\hat{X}_{2\varphi}.$$

As a result, the control law applied to the vertical displacement of the chassis and the roll angle, respectively, is given by

$$u_i=-\frac{1}{\hat{b}_{0i}}(K_{pi}(y_i-y_{ri})+K_{di}\dot{\hat{y}}_i+\hat{f}_i),\ i=\{z,\ \varphi\},\quad(10)$$

where

$$K_{pz}=K_{p\varphi}=\frac{10}{3T_p^2}\text{ and }K_{dz}=K_{d\varphi}=\frac{5}{2T_p}.\quad(11)$$

The closed-loop pole and damping factor of the ADRC system can be calculated as follows:

$$K_p=w_{CL}^2,\ K_d=2\xi w_{CL}$$
$$\Rightarrow -w_{CL}=-\sqrt{K_p},\ \xi=0.5\frac{K_d}{\sqrt{K_p}}.\quad(12)$$

Hence, the entire system has the characteristic equation $\Delta(s)=s^2+K_d s+K_p$, being Hurwitz stable if $K_p,\ K_d>0.$ These conditions hold under $T_p>0$.

If the ADRC law in the heave and roll loops is given by (10), the control coefficients by (11), and the observer coefficients by (12), the entire system will be stable. In this case, the control loop of the pitch angle has another ADRC law with empirically chosen parameters. Figure 6 shows the diagram of the closed loop system.

The control distribution mechanism is a *decoupling matrix* with stabilizing forces for the heave, pitch, and roll angles. This mechanism outputs the control forces for the suspension of the four corners of the vehicle. In view of (2), the distribution mechanism can be represented as follows:

$$K=\mathrm{Pinv}\left(\begin{bmatrix} 1 & 1 & 1 & 1 \\ a & a & -b & -b \\ w_f & -w_f & w_r & -w_r \end{bmatrix}\right),$$

where Pinv denotes matrix pseudoinverse.

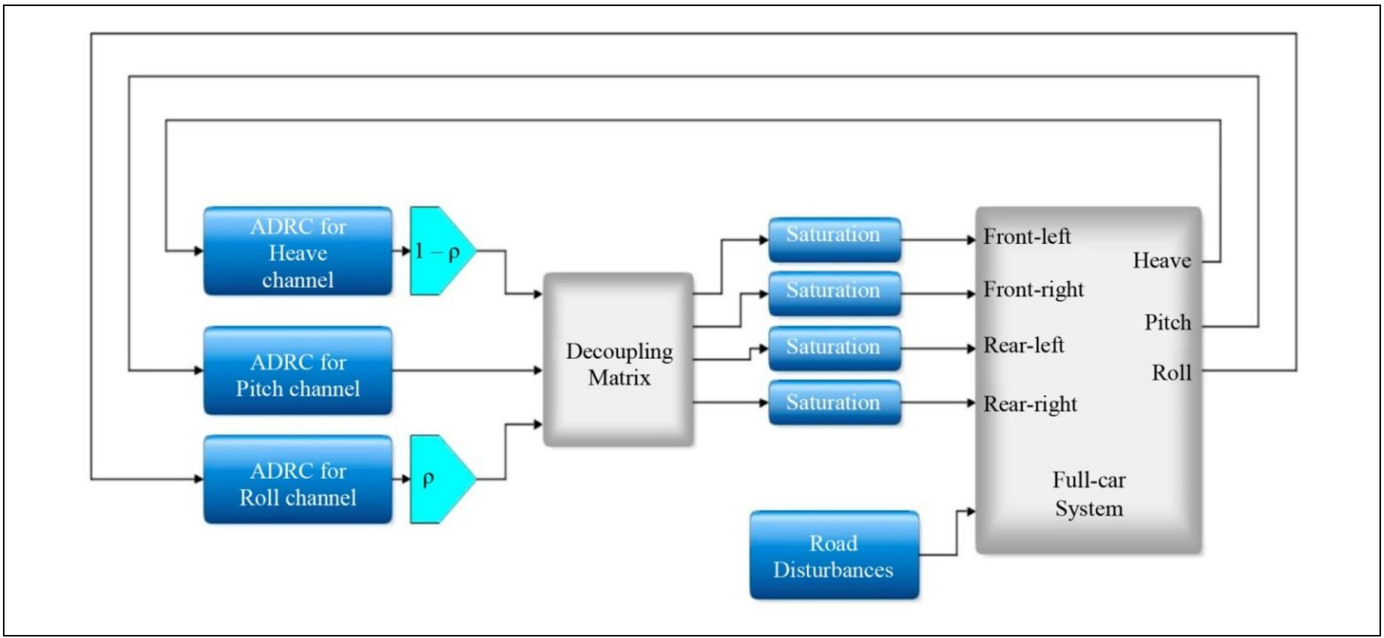

Fig. 6. The full car model with a suspension controlled by the optimized ADRC law.

5. SIMULATION RESULTS

The proposed control strategy was tested under the following assumptions: the road bumps meet the ISO 8608 standard for Class D roads and the vehicle speed varies between 20 and 70 km/h.

During the testing procedure, we calculated the PSDs of the sprung mass acceleration and roll angle for 1000 seconds of operation. The comfort and handling indices were calculated by formulas (3) and (4), respectively.

The first stage was to study variations of the comfort and handling indices for different values of the control coefficient ρ under a fixed vehicle speed of 54 km/h. This stage yields a balance value ρ, characterizing the handling–comfort trade-off.

The second stage was to study variations of the comfort and handling indices for different values of the vehicle speed under the balance value ρ.

According to the ISO 2631-1 standard, a ride is considered comfortable if the RMS value of the sprung mass acceleration is below 0.31 m/s^2. According to the criterion proposed in this paper, the required degree of handling is achieved if the value of (4) is less than 3.00×10^{-4}.

Table 3 presents the variations of the comfort and handling indices for different values ρ.

Figure 7 shows the normalized values of the comfort and handling indices in the range [0, 1]. Clearly, the trade-off corresponds to the point ρ = 0.4.

Choosing ρ = 0.4, we also studied the variations of the comfort and handling indices for different vehicle speeds (Table 4).

Table 3

Comfort and handling indices for different values ρ

ρ	Comfort index	Handling index
0.1	0.1653	5.00×10^{-4}
0.2	0.1786	3.14×10^{-4}
0.3	0.1921	2.33×10^{-4}
0.4	0.2051	1.48×10^{-4}
0.5	0.2164	1.51×10^{-4}
0.6	0.2243	1.26×10^{-4}
0.7	0.2287	1.08×10^{-4}
0.8	0.2566	0.96×10^{-4}
0.9	0.5153	1.04×10^{-4}

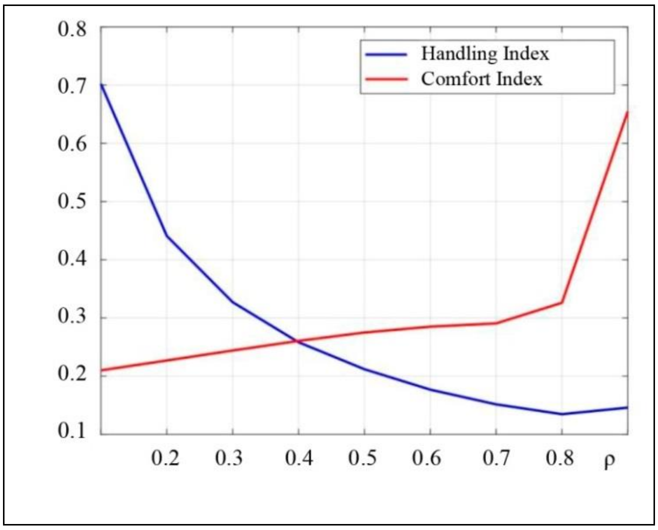

Fig. 7. Normalized values of the comfort and handling indices in the range [0, 1].

Table 4

Comfort and handling indices for different vehicle speeds

Vehicle speed, km/h	Comfort index		Handling index	
	Active suspension	Passive suspension	Active suspension	Passive suspension
20	0.1248	0.4169	0.68×10^{-4}	4.82×10^{-4}
30	0.1529	0.5106	1.02×10^{-4}	7.23×10^{-4}
40	0.1765	0.5896	1.36×10^{-4}	9.65×10^{-4}
50	0.1974	0.6592	1.70×10^{-4}	12.0×10^{-4}
60	0.2162	0.7221	2.04×10^{-4}	14.0×10^{-4}
70	0.2341	0.7800	2.42×10^{-4}	17.0×10^{-4}
80	0.2511	0.8338	2.89×10^{-4}	19.0×10^{-4}
90	0.2669	0.8844	3.45×10^{-4}	22.0×10^{-4}
100	0.2868	0.9323	4.26×10^{-4}	24.0×10^{-4}

According to Table 4, the proposed algorithm works fine up to a vehicle speed of 80 km/h. However, riding the car at speeds above 30 km/h in these conditions would be dangerous in the passive suspension case.

The proposed algorithm can be used to switch between different operation modes by adjusting one coefficient.

CONCLUSIONS

This paper has presented an optimization procedure for managing the handling–comfort trade-off in the full car model. The algorithm is based on selecting ADRC parameters using a quality criterion with two characteristics, balancing between them by adjusting one coefficient. According to the results, this trade-off management process is uncomplicated and practicable. The effectiveness of this approach has been demonstrated for a vehicle moving on a class D road (ISO 8608) with a speed varying from 20 to 80 km/h. The most important features of this approach are the simple choice of controller parameters and the ease of application. This algorithm cannot be attributed to Model Predictive Control since the control signal is not included in the quality criterion.

REFERENCES

1. Liu, H., Gao, H., and Li, P., *Handbook of Vehicle Suspension Control System*, Institution of Engineering and Technology, 2013.
2. Alhelou, M. and Gavrilov, A.I., Managing the Handling–Comfort Contradiction of a Quarter-Car System Using Kalman Filter, *Transactions of the Institute of Measurement and Control*, 2021, no. 43(10), pp. 2292–2306.
3. Alhelou, M. and Gavrilov, A.I., Unscented Kalman-filter to Manage the Handling-Comfort Trade-off of Quarter-of-Vehicle, *Transactions of the Institute of Measurement and Control*, 2021, vol. 44, iss.1, art. ID 01423312211031774.
4. Pepe, G., Roveri, N., and Carcaterra, A., Experimenting Sensors Network for Innovative Optimal Control of Car Suspensions, *Sensors*, 2019, vol. 19, iss. 14, art. no. 3062.
5. Franz, D., Simulink Control Model of an Active Pneumatic Suspension System in Passenger Cars, *Master of Science in Mechatronic Engineering Thesis*, Politecnico di Torino, 2019.
6. Els, P.S., Theron, N.J., Uys, P.E., and Thoresson, M.J., The Ride Comfort vs. Handling Compromise for Off-road Vehicles, *Journal of Terramechanics*, 2007, vol. 44, no. 4, pp. 303–317.
7. Shirahatti, A., Prasad, P., Panzade, P., and Kulkarni, M., Optimal Design of Passenger Car Suspension for Ride and Road Holding, *Journal of the Brazilian Society of Mechanical Sciences and Engineering*, 2008, no. 30, pp. 66–76.
8. Darus, R., and Sam, Y.M., Modeling and Controlling Active Suspension System for a Full Car Model, *Proceedings of 2009 5th International Colloquium on Signal Processing & Its Applications*, Kuala Lumpur, 2009, pp. 13–18.
9. Gohrle, C., Wagner, A., Schindler, A., and Sawodny, O., Active Suspension Controller Using MPC Based on a Full-car Model with Preview Information, *Proceedings of 2012 American Control Conference (ACC)*, Montreal, 2012, pp. 497–502.
10. Nguyen, M. Q., Canale, M., Sename, O., and Dugard, L., A Model Predictive Control Approach for Semi-active Suspension Control Problem of a Full Car, *Proceedings of 2016 IEEE 55th Conference on Decision and Control (CDC)*, Las Vegas, 2016, pp. 721–726.
11. Verschueren, R., Zanon, M., Quirynen, R., and Diehl, M., Time-Optimal Race Car Driving Using an Online Exact Hessian Based Nonlinear MPC Algorithm, *Proceedings of 2016 European Control Conference*, Aalborg, 2016, pp. 141–147.
12. Rizvi, S.M.H., Abid, M., Khan, A.Q., et al., H_∞ Control of 8 Degrees of Freedom Vehicle Active Suspension System, *Jour-*

nal of King Saud University-Engineering Sciences, 2018, vol. 30, no. 2, pp. 161–169.
13. Van der Sande, T.P.J., Gysen, B.L.J., Besselink, I.J.M., et al., Robust Control of an Electromagnetic Active Suspension System: Simulations and Measurements, *Mechatronics*, 2013, vol. 23, no. 2, pp. 204–212.
14. Wang, C., Deng, K., Zhao, W., et al., Robust Control for Active Suspension System under Steering Condition, *Science China Technological Sciences*, 2017, vol. 60, no. 2, pp. 199–208.
15. Alhelou, M., Wassouf, Y., and Gavrilov, A.I., Linear-Control vs. ADRC for Automatic Management of the Handling-Comfort Contradiction of a Quarter-Car System, *International Journal of Heavy Vehicle Systems*, 2022, vol. 29, no. 2, pp. 145–162.
16. Alhelou, M., Wassouf, Y., Serebrenny, V.V., et al., Managing the Handling-Comfort Trade-Off of a Quarter Car Suspension System Using Active Disturbance Rejection Control and Vyshnegradsky Equation, *Mekhatronika, Avtomatizatsiya, Upravlenie*, 2022, vol. 23, no. 7, pp. 367–375.
17. Kumar, S., Medhavi, A., and Kumar, R., Modeling of an Active Suspension System with Different Suspension Parameters for Full Vehicle, *Indian Journal of Engineering and Materials Sciences (IJEMS)*, 2021, vol. 28, no. 1, pp. 55–63.
18. Alhelou, M., Wassouf, Y., Serebrenny, V.V., et al., The Handling-Comfort Trade-Off in a Quarter-Car System: Automatic Adaptive Management via Active Disturbance Rejection Control, *Control Sciences*, 2022, no. 2, pp. 29–39.
19. Gao, Z., and Tian, G., Extended Active Disturbance Rejection Controller, US Patent 8180464, 2012.

This paper was recommended for publication by S.A. Krasnova, a member of the Editorial Board.

Received June 8, 2022,
and revised December 14, 2022.
Accepted January 25, 2023.

Author information

Alhelou, Muhammed. Postgraduate, Bauman Moscow State Technical University, Moscow, Russia
✉ muhammed.alhelou@gmail.com

Wassouf, Yazan. Postgraduate, Bauman Moscow State Technical University, Moscow, Russia; chief programmer of unmanned vehicles, KAMAZ Innovations Center, Moscow, Russia
✉ vassufya@student.bmstu.ru

Korzhukov, Maksim Valentinovich. KAMAZ Innovations Center, Moscow, Russia
✉ KorzhukovMV@kamaz.ru

Lobusov, Evgeny Sergeevich. Cand. Sci. (Eng.), Bauman Moscow State Technical University, Moscow, Russia
✉ evgeny.lobusov@yandex.ru

Serebrenny, Vladimir Valer’evich. Serebrenny Vladimir Valer'evich. Sci. (Eng.), Bauman Moscow State Technical University, Moscow, Russia
✉ vsereb@bmstu.ru

Cite this paper
Alhelou, M., Wassouf, Y., Korzhukov, M.V., Lobusov, E.S., and Serebrenny, V.V., Managing the Handling–Comfort Trade-Off in the Full Car Model by Active Suspension Control. *Control Sciences* **1,** 36–47 (2023). http://doi.org/10.25728/cs.2023.1.5

Translated into English by *Alexander Yu. Mazurov*,
Cand. Sci. (Phys.–Math.),
Trapeznikov Institute of Control Sciences,
Russian Academy of Sciences, Moscow, Russia
✉ alexander.mazurov08@gmail.com